

Relevance of the coal rank on the performance of the in-situ Gasification Chemical-Looping Combustion

A. Cuadrat, A. Abad*, F. García-Labiano, P. Gayán, L.F. de Diego, J. Adánez

Instituto de Carboquímica (ICB-CSIC), Dept. of Energy & Environment, Miguel Luesma Castán 4, 50018-Zaragoza, Spain

* Corresponding author: Tel: (+34) 976 733 977. Fax: (+34) 976 733 318. E-mail address: abad@icb.csic.es (A. Abad)

Abstract

In this work the CLC process for solid fuels using ilmenite as oxygen carrier was evaluated in a continuous CLC unit. In this process, gasification of solid fuel happens in the fuel reactor which is fluidized by a gasifying agent, i.e, H₂O. This process has been referred as in-situ Gasification CLC, iG-CLC. The feasibility of using fuels ranging from lignite to anthracite and the effect of the coal rank on the process performance was evaluated. The carbon capture efficiency followed the trend of the coal rank, as it was higher for lignite, then for the bituminous coals and it was lower for anthracite. Special attention was put on the combustion of the volatile matter of the different fuels. In all cases oxygen demands lower than 10% were found; for anthracite the oxygen demand values were 3.5% because of the lower volatile content of this fuel. A temperature increase was proven to be advantageous to reach high carbon capture and combustion efficiencies for all the fuels tested. Also, the feasibility of using H₂O:CO₂ mixtures as gasification agent with each type of fuel was also assessed and it was seen that in case of bituminous coals and lignite some of H₂O can be replaced by CO₂.

Keywords: Chemical-looping combustion, Oxygen carrier, Ilmenite, CO₂ capture, Coal.

1. Introduction

CO₂ is considered the gas making the largest contribution to the global warming. Its concentration in the atmosphere has increased strongly over the few past decades as a result of the dependency on fossil fuels for energy production. The global atmospheric concentration of CO₂ has increased up to 390 ppm in 2010 [1]. The abatement of greenhouse gas emissions can be achieved through a wide portfolio of measures in the energy, industry, agricultural and forest sectors. According to the analysis made by the IPCC and IEA [2,3], Carbon Capture and Storage could contribute 15–55% to the cumulative mitigation effort worldwide until 2100, to mitigate climate change at a reasonable cost.

In this context, Chemical-Looping Combustion (CLC) is one of the most promising technologies to carry out CO₂ capture at a low cost [4]. CLC is based on the transfer of the oxygen from air to the fuel by means of a solid oxygen carrier. Different configurations have been proposed for CLC: interconnected fluidized beds [5] and fixed alternating beds [6,7]. The most used for solid fuel combustion is the two interconnected fluidized beds configuration [8-17], for which the two reactors are the fuel and the air reactor. In the fuel reactor the oxygen carrier is reduced through oxidation of the fuel, thus obtaining a gas stream composed of CO₂ and H₂O. The oxygen carrier is afterwards directed to the air reactor, where it is re-oxidized with air and regenerated to start a new cycle. The net chemical reaction is the same as at usual combustion with the same combustion heat released, but with the advantage of the intrinsic CO₂ separation in the process without an additional step.

The development of clean coal conversion processes is of great interest regarding the intensive use of coal as energy source. In this sense, the use of CLC with solid fuels, e.g. coal, is very interesting when the capture of CO₂ is considered for a clean coal conversion process. One of the options for CLC with solid fuels is to introduce the fuel directly in the fuel reactor,

where it is mixed with the oxygen carrier and being gasified by the fluidizing gas, i.e. H₂O or CO₂ [18], see scheme in Fig. 1. This process has been later denoted as the in-situ Gasification Chemical Looping Combustion process (iG-CLC) [19]. An optional stream is also drawn in Fig. 1 to indicate that some CO₂ from the fuel reactor outlet flow could be recirculated and used to fluidize the fuel reactor. Recirculation of CO₂ could be advantageous from an energetic point of view.

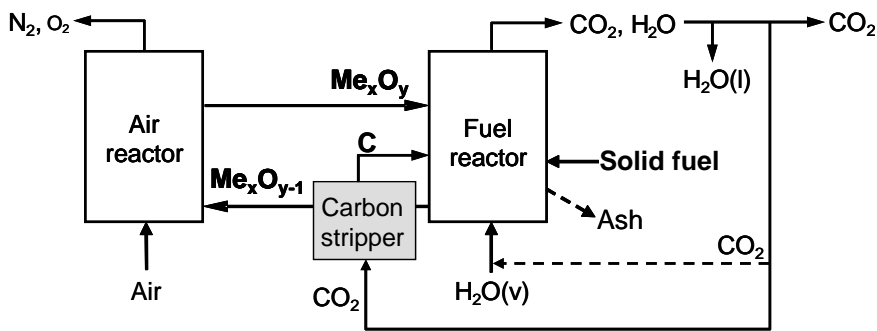
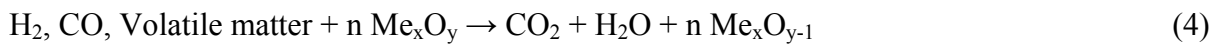


Fig. 1. Reactor scheme of the CLC with solid fuels process. (--- optional stream).

Thereby, the solid fuel devolatilizes and the char gets gasified following reactions (1-3). The oxidized oxygen carrier, Me_xO_y, reacts simultaneously with the gaseous products of the solid fuel devolatilization and gasification, with H₂ and CO as main components to give the combustion products, CO₂ and H₂O (see Eq. 4). Then the reduced oxygen carrier, Me_xO_{y-1}, exits the fuel reactor and is oxidized with air in the air reactor according to reaction (5).



To find suitable oxygen carriers is a key factor for the development of the CLC technology. An oxygen carrier should have, during many cycles, high selectivity towards CO₂ and H₂O, enough oxygen transport capacity, high reactivity in reduction and oxidation, mechanical resistance, low attrition rate and show no agglomeration problems. For the use of CLC with solid fuels, since part of the oxygen carrier is expected to be removed mixed with fuel ashes, it would be desirable that the oxygen carrier was environmentally friendly and of low cost. Therefore natural minerals [17, 20], industrial residues [21, 22] or synthetic carriers made with low-cost raw materials [23] are of great interest. Ilmenite was found to be an appropriate material for its use as oxygen carrier in CLC with solid fuels [8-11]. Ilmenite is a relatively cheap and abundantly occurring mineral mainly consisting of FeTiO₃.

In previous CLC experiments with solid fuels performed to date, full oxidation of the outlet fuel reactor stream could not be achieved [8-17]. Furthermore, the extent of unburnt gases was similar as if a highly Ni-based oxygen carrier was used [14-16]. Therefore, in order to oxidize completely unburnt compounds to CO₂ and H₂O and enhance combustion, an oxygen polishing step downstream was proposed, that is, injection of pure oxygen to the gas flow after the fuel reactor cyclone [8,9], with the corresponding oxygen demand.

The gasification process has been identified as the controlling step in this process [24-27]. Leion et al. [28] saw in a batch fluidized-bed reactor with various bituminous coals and petcoke that the oxygen carrier enhances the gasification rate of the solid fuel because the presence of oxygen carrier particles reduces the fraction of H₂ in the bed, which has an inhibitory effect on the gasification. This fact has been observed as much for steam gasification as for CO₂ gasification using different oxygen carrier materials, for solid fuels such as bituminous coals or lignites [27-30]. Char gasification is usually a slow process and the solids stream exiting from the fuel reactor could contain some unconverted char together with the oxygen carrier [12,13]. Thus, total CO₂ capture efficiency cannot be reached when

using solid fuels if there is by-pass of non-gasified char particles to the air reactor. The use of a carbon separation system, for instance a carbon stripper, has been proposed to carry out the separation of char from the oxygen carrier and later to be re-introduced to the fuel reactor, thus reducing the amount of carbon transferred from the fuel to the air reactor [18]. Berguerand et al. designed and built a 10 kW_{th} CLC plant that included a carbon stripper [9]. Char conversion was seen to be related to the reactivity of the solid fuel particles [28], lowering the influence of the oxygen carrier's reactivity. TGA tests done with a synthetic Cu-based oxygen carrier and a sub-bituminous coal, wood and a low-density polyethylene as fuels showed the feasibility of using solid fuels with higher reactivity, that is, higher volatile matter, for this technology [18]. Linderholm et al. [31] studied the fuel conversion in a batch fluidized bed reactor for five fuels using ilmenite as oxygen carrier and found that in all cases the fuel conversion were promoted with the temperature. Depending on the type of fuel, the fuel conversion rates at 1030°C were 1.6 to 3.2 times higher than the corresponding rates at 970°C. They also found that three bituminous coals had similar char conversion rates, and it was much slower for a petroleum coke, followed by a metallurgical coke. Dennis et al. also found differences in the conversion of char, depending on the type of fuel when lignite or bituminous coals were used as fuels [29,30].

As for continuous operation, Berguerand and Lyngfelt [8-11] used a 10 kW_{th} chemical-looping combustor with ilmenite as oxygen carrier and South African coal and petroleum coke as solid fuels. They analyzed the combustion process focusing on char conversion and the conversion of gases from steam gasification (CO and H₂) was analyzed. A CO₂ capture within the range 65-82% was obtained for South African coal as fuel at 900-950°C. The incomplete gas conversion resulted in the presence of unconverted gases in the fuel reactor outlet stream (CO, H₂ and CH₄) that demanded 29-30% of the total oxygen needed to fully burn the solid fuel to H₂O and CO₂. They analyzed mainly the temperature as one of the main

process parameters affecting the system performance, being higher efficiencies reached at high temperatures. Temperatures above 1000 °C were tested in some cases [10]. In those experiments oxygen demands of 27-36% were found, for which 5-9% corresponded to the oxygen demand for char combustion. Average carbon capture efficiencies of 80% were obtained in all the experimental works at high temperatures with petcoke, which is a fuel with low volatile content.

Biomass as solid fuel was evaluated by Shen et al. [32] in a continuous 10 kW_{th} CLC combustor using an oxygen carrier prepared from iron oxide and CO₂ as gasification medium. Gu et al. [33] also proved the feasibility of using CLC for both biomass and a biomass/coal mixture as solid fuels in a continuous 1 kW_{th} CLC facility and using an Australian iron ore as oxygen carrier. They found that the difference in the carbon capture efficiency between the biomass and the biomass/coal mixture, was caused by the combustible carbonaceous gases in the fuel reactor. It was 98% above 800°C for biomass and 93-98% at 900-985°C for the biomass/coal mixture. The blend of biomass with coal was proposed as an effective measure to reduce the potential negative influence of the alkali metals of biomass ash on the performance of oxygen carriers.

In this work the feasibility of the iG-CLC process for different types of coals using ilmenite as oxygen carrier was evaluated in a continuous CLC unit. Fuels ranging from lignite to anthracite were used. The effect of the coal rank on the process performance was assessed. The temperature as one of the main parameters of influence was analyzed for all the fuels tested. The feasibility of using H₂O:CO₂ mixtures as gasification agent with each type of fuel was also studied. The effect of the main process parameters on char conversion and combustion efficiency was analyzed. Special attention was put on the combustion of the volatile matter of the different fuels, since to date no research has been done on the combustion of devolatilization products.

2. Experimental section

2.1. Bed material and fuel

Ilmenite has been one of the most used materials for combustion of solid fuels in iG-CLC [8-13,34]. The bed material in this study was a Norwegian ilmenite. Ilmenite is a common mineral found in metamorphic and igneous rocks. The ilmenite used is a concentrate from a natural ore. Fe_2O_3 and Fe_2TiO_5 are the active phases that behave as the oxygen carrier. The oxygen carrier had been initially sieved to a particle size of +150-300 μm and particles were pre-oxidized at 950 °C in air during 24 h. Considering an average particle diameter of 212 μm , the minimum fluidization velocity of the used ilmenite particles was calculated to be 0.024 m/s at 900°C. Ilmenite undergoes an activation process which was deeply studied in previous works [35,36]. The batch of ilmenite used in these experiments was previously used in continuous tests using Colombian coal as fuel and it was fully activated [12,13]. Thereby, ilmenite particles showed constant reactivity during all the experiments. Table 1 shows the main physical and chemical properties of pre-oxidized ilmenite and the activated ilmenite used in these experiments. The procedure to obtain the physic-chemical characteristics has been described previously [36].

Table 1. Main properties of pre-oxidized and activated ilmenite particles.

| | Pre-oxidized ilmenite | Activated ilmenite |
|---|--|--|
| XRD phases | $\text{Fe}_2\text{TiO}_5, \text{Fe}_2\text{O}_3, \text{TiO}_2$ | $\text{Fe}_2\text{TiO}_5, \text{Fe}_2\text{O}_3, \text{TiO}_2$ |
| Crushing strength (N) | 2.2 | 2.0 |
| Oxygen transport capacity(%) | 4.0 | 3.9 |
| Skeletal density (kg/m^3) | 4100 | 4200 |
| Porosity (%) | 1.2 | 18 |
| BET Surface (m^2/g) | 0.8 | 0.4 |

The oxygen transport capacity, which is the mass fraction of the solid material that can be used in the oxygen transfer, was measured to be 3.9% for the CLC process. Note that the oxygen transport capacity and the crushing strength for particles used a total of 98 hours in continuous operation were very similar to the values for unused particles. In this process the oxidized species Fe_2TiO_5 and Fe_2O_3 transfer oxygen by getting reduced to FeTiO_3 and Fe_3O_4 , respectively. The ilmenite used was composed of 11.7% Fe_2O_3 , 53.2% Fe_2TiO_5 and 29.5% TiO_2 .

Table 2. Proximate and ultimate analysis and lower heating value, LHV, of coals used in this work.

| | Lignite | HV Bit. Colombian | MV Bit. S.African | Anthracite |
|------------------------|---------|-------------------|----------------------|------------|
| Moisture (wt.%) | 12.5 | 2.3 | 4.2 | 1 |
| Volatile matter (wt.%) | 28.7 | 33 | 25.5 | 7.6 |
| Fixed carbon (wt.%) | 33.6 | 55.9 | 56 | 59.9 |
| Ash (wt.%) | 25.2 | 8.8 | 14.3 | 31.5 |
| LHV (kJ/kg) | 16250 | 21900 | 26435 | 21880 |
| C (wt.%) | 45.4 | 65.8 | 69.3 | 60.7 |
| H (wt.%) | 2.5 | 3.3 | 3.5 | 2 |
| N (wt.%) | 0.5 | 1.6 | 2 | 0.9 |
| S (wt.%) | 5.2 | 0.6 | 1 | 1.3 |
| O (wt.%) | 8.6 | 17.6 | 5.7 | 2.4 |

A range of coals with different rank was used as fuels: a Spanish anthracite, a Spanish lignite and two bituminous coals from Colombia and South Africa. Following the ASTM characterization, South African coal is a medium volatile (MV) bituminous coal, whereas Colombian coal is a high volatile (HV) bituminous coal. The coal particle size for all coals tested was +200-300 μm . Ultimate and proximate analyses and lower heating values of the used coals as received are gathered in Table 2. The high volatile bituminous Colombian coal used had been subjected to a thermal treatment at 180°C that eliminated the swelling properties seen in this fuel, which prohibited its use in our CLC unit because of the small size of the screw-feeder. Due to this pre-treatment the coal gets partially pre-oxidized, which is shown by its high oxygen content. The pre-treatment led to a slight change in the reactivity of the fuel [12]. Its properties are also included in Table 2.

2.2. ICB-CSIC-s1 facility for CLC with coal

A schematic view of the plant is shown in Fig. 2. The set-up was basically composed of two interconnected fluidized-bed reactors joined by a loop seal, a riser for solids transport from the air reactor to the fuel reactor, a cyclone and a solids valve to control the flow rate of solids fed to the fuel reactor. This design allowed the measure and the control of the solid circulation flow rate between both reactors. The total ilmenite inventory in the system was 3.5 kg and the solids inventory in the fuel reactor was 0.8 kg ilmenite. This facility has been used in continuous operation in previous studies with El Cerrejón bituminous Colombian coal as fuel [12,13].

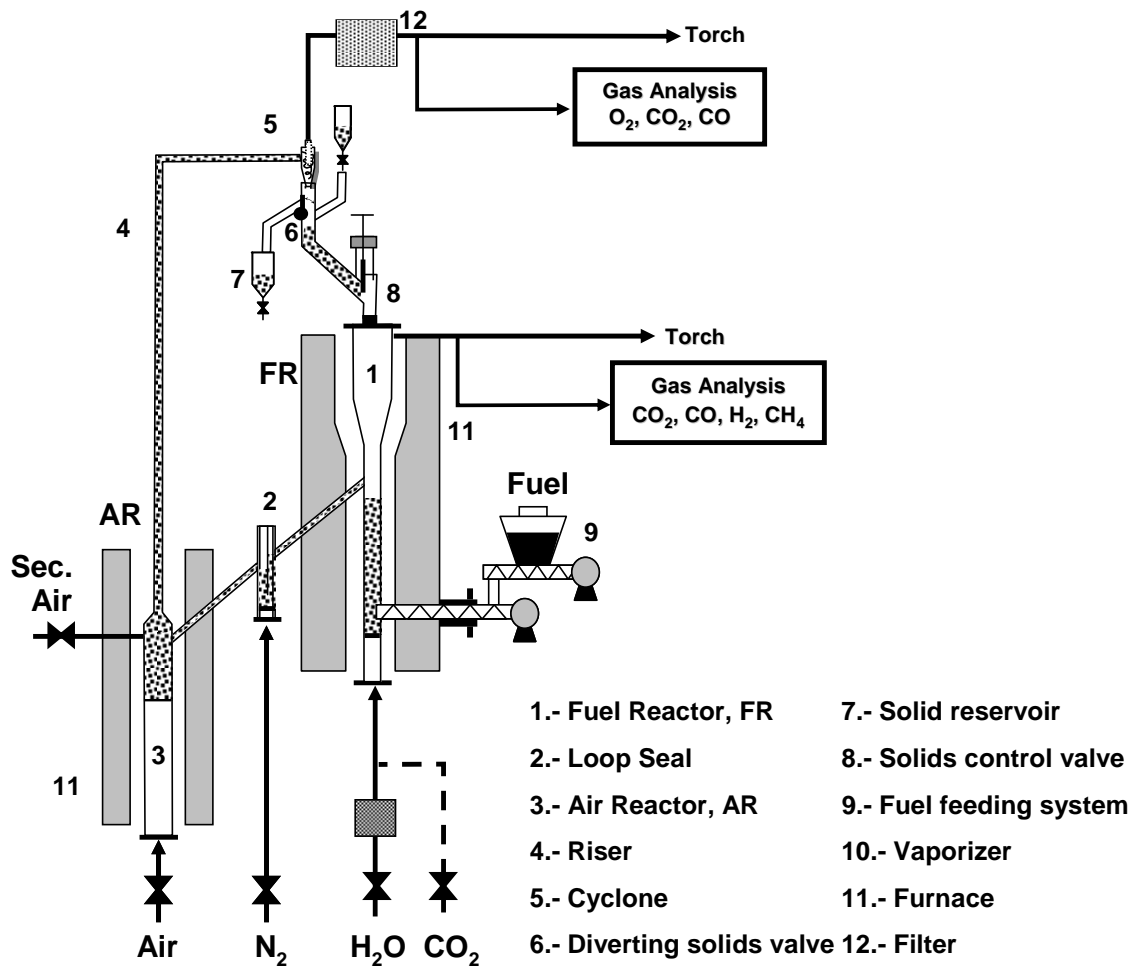


Fig. 2. Schematic diagram of the ICB-CSIC-s1 facility for coal-fuelled CLC.

The fuel reactor consisted of a bubbling fluidized bed with 50 mm of inner diameter and 500 mm height, being 200 mm the height of the solids bed. The fluidizing gas was composed of H₂O:CO₂ mixtures, which acts also as gasifying agent. The gasification agent flow was 190 L_N/h. Coal is fed by a screw feeder placed just above the fuel reactor distributor plate in order to maximize the time that the fuel and volatile matter are in contact with the bed material. The screw feeder has two steps: the first one with variable speed to control the coal flow rate, and the second has high rotating velocity to avoid coal pyrolysis inside the screw. A small N₂ flow of 18 L_N/h is fed at the beginning of the screw-feeder to avoid possible volatile reverse flow or entrance of steam. In the fuel reactor the oxygen carrier is reduced by the volatile matter and gasification products of coal. Reduced oxygen carrier particles overflowed into the air

reactor through a U-shaped fluidized bed loop seal with an inner diameter of 50 mm. The loop-seal was fluidized with 90 L_N/h of N₂. Thus, gas mixing between the fuel and air reactors was avoided. The oxidation of the carrier took place in the air reactor, consisting of a bubbling fluidized bed with 80 mm of inner diameter and 100 mm bed height, and followed by a riser of 30 mm inner diameter. The gas flows introduced in the air reactor were 2100 L_N/h as primary air and 400 L_N/h of secondary air at the top of the bubbling bed to help particle entrainment. N₂ and unreacted O₂ left the air reactor and went through a high-efficiency cyclone and a filter before the stack. The oxidized solid particles recovered by the cyclone were sent to a solids reservoir, which acts as a loop seal, setting the oxygen carrier ready to start a new cycle. The regenerated oxygen carrier particles returned to the fuel reactor by gravity from the solids reservoir through a solids valve which controlled the flow rates of solids entering the fuel reactor. A diverting solids valve located below the cyclone allowed the measurement of the solids flow rates at any time.

Because of its small size, the system is not auto-thermal and is heated up with various ovens to get independent temperature control of the air reactor, fuel reactor, and fuel reactor freeboard. During operation, temperatures in the bed and freeboard of the fuel reactor, air reactor bed and riser were monitored as well as the pressure drops in important locations of the system, such as the fuel reactor bed, the air reactor bed and the loop seal.

CH₄, CO and CO₂ concentrations in the fuel reactor stream were continuously measured by nondispersive infrared (NDIR) analyzers (Maihak S710/UNOR, Siemens Ultramat/Oxymat 6) and H₂ concentration by a thermal conductivity detector (Maihak S710/THERMOR). CO, CO₂ and O₂ concentrations in the fuel reactor were determined by a combined NDIR-paramagnetic analyzer (Siemens Ultramat/Oxymat 6). All data were collected by means of a data logger connected to a computer.

In some selected experiments, GC analysis of the outgoing fuel reactor gases was done to measure possible hydrocarbons, and possible tar formation was also measured following the tar protocol [37].

Table 3 shows the conditions for the series of experiments carried out. The fuel reactor temperature was varied within the range 850-930°C. But in all the experiments, the temperature in the air reactor was kept at 930°C, being 900°C in the fuel reactor freeboard. In the riser the temperature was from 900°C at the bottom to 750°C at the top. Most experiments were done with steam as fluidization agent in the fuel reactor, and H₂O:CO₂ mixtures were also used as fluidization agents in a series of tests. The gas velocity in the fuel reactor was 0.12 m/s at 900°C, which corresponded to around 5 times the minimum fluidization velocity of the particles. However, a previous study showed that the effect of the gasification agent flow was negligible for ratios steam to fixed carbon over 1 [13]. The gas velocity in the air reactor was 0.1 m/s and the velocity in the air reactor riser was 4.3 m/s at a temperature of 900 °C. The average solids circulation flow was 3.0 kg/h for all fuels tested. This means that the oxygen carrier to fuel ratio was 1.1 in all cases. At least every condition was maintained stable during 30 minutes. Coal was fed for 13 hours using lignite, 7 hours using bituminous South African coal and 11 hours using anthracite. In total, 44 hours of continuous operation of hot conditions were carried out. An experiment previously performed with Colombian bituminous coal “El Cerrejón” which was done with similar solids residence time and solids inventory is also included. A deeper study on “El Cerrejón” coal as fuel used in iG-CLC can be found elsewhere [12,13].

To do a more complete study on the gasification rates for the different coals under well defined conditions, the char conversions reached with time were measured by TGA at 950°C. The samples were heated up to the desired temperature in N₂ and when the volatiles had been

released and the weight of the sample was stable, the remaining char was gasified with steam with a 50 vol.%H₂O+50 vol.%N₂ mixture.

Table 3. Conditions for the series of experiments with variation of the fuel reactor temperature and variation of the gasification agent type (H₂O:CO₂ mixtures) with the different types of coals tested, i.e, lignite, bituminous South African coal and anthracite. The conditions of a previous test done with Colombian bituminous coal is also included [13].

| Effect of the temperature | | | | | |
|---|----------------------|-----------------|---|--|-------------------------------|
| Coal type | T _{FR} (°C) | Coal feed (g/h) | $\frac{\text{Gasif.agent}}{\text{Fixed C}}$ (mol/mol) | H ₂ O (vol.%) in the gasification mixture | Fuel power (W _{th}) |
| Lignite (Spain) | 870-920 | 100 | 3.0 | 100 | 450 |
| MV Bituminous (S. Africa) | 850-915 | 79 | 2.3 | 100 | 580 |
| Anthracite (Spain) | 870-930 | 94 | 1.8 | 100 | 570 |
| HV Bituminous (Colombia) | 890 | 83 | 2.2 | 100 | 505 |
| Effect of the gasification mixture H ₂ O:CO ₂ | | | | | |
| Coal type | T _{FR} (°C) | Coal feed (g/h) | $\frac{\text{Gasif.agent}}{\text{Fixed C}}$ (mol/mol) | H ₂ O (vol.%) in the gasification mixture | Fuel power (W _{th}) |
| Lignite (Spain) | 920 | 100 | 3.0 | 100;60;0 | 450 |
| MV Bituminous (S. Africa) | 910 | 79 | 2.3 | 100;58;0 | 580 |
| Anthracite (Spain) | 925 | 94 | 1.8 | 100;48;0 | 570 |

3. Data evaluation

The evaluation of the fuel reactor performance is carried out by the analysis of two main parameters: the carbon capture efficiency and the combustion efficiency in the fuel reactor. The purpose of the data evaluation is to assess the performance of the process in the different experiments, using the measured values of the gas concentrations, temperatures and solid

circulation rates. The absence of a carbon separation system facilitates the interpretation of the effect of the operational conditions on the results obtained, as the solids mean residence time can be easily calculated. Otherwise, the presence of a carbon separation system would increase the mean residence time of char particles to an unknown value.

As it was seen in previous experiments [12], there is some elutriation of char in this facility with coal. Thus, the sum of carbon measured in the gases coming from the fuel reactor and the air reactor is less than the carbon in the coal feeding flow. However, in case of an industrial plant the possible elutriated char will be collected by a cyclone and reintroduced in the fuel reactor. The total effective carbon introduced in the facility for particle size of +200-300 μm was 89% for lignite, 94% for Colombian coal, 77% for South African and 87% for anthracite. All calculations and analyses in this study are made considering only the effective char, that is, the introduced char that had not been elutriated from the fuel reactor. Thus, the balance to carbon atoms was done by considering the carbon exiting the fuel reactor as gases (CO_2 , CO and CH_4) and the carbon in the char being conveyed to the air reactor, where it is burnt with air and detected as CO_2 .

The efficiencies that indicate the performance of the process are defined as follows. The carbon capture efficiency is the physical removal of carbon dioxide that would otherwise be emitted into the atmosphere. Getting high carbon capture efficiency during energy generation is the motivation of this technology. The carbon capture efficiency, η_{CC} , is here defined as the fraction of the carbon introduced that is converted to gas in the fuel reactor. The carbon captured in the system is the carbon contained in the volatiles plus the carbon in the char that is gasified. For the experiments using CO_2 as fluidization agent in the fuel reactor, the inlet CO_2 flow must be subtracted. Thus, the carbon capture efficiency depends on the fraction of char that has been gasified, and it is calculated as:

$$\eta_{CC} = \frac{[F_{CO_2,FR} + F_{CO,FR} + F_{CH_4,FR}]_{out} - [F_{CO_2,FR}]_{in}}{[F_{CO_2,FR} + F_{CO,FR} + F_{CH_4,FR} + F_{CO_2,AR}]_{out} - [F_{CO_2,FR}]_{in}} \quad (6)$$

$F_{CO_2,FR}$, $F_{CH_4,FR}$ and $F_{CO,FR}$ being the flows in the fuel reactor of CO_2 , CH_4 , and CO . The carbon of the unreacted char flowing towards the air reactor is the CO_2 gas flow in the air reactor, $F_{CO_2,AR}$. The gaseous flows are calculated by a balance of the N_2 flows exiting from the fuel reactor, which comes from the N_2 introduced into the screw-feeder and the fraction of the N_2 flow fed into the loop seal. Previous experiments were done by feeding CO_2 into the loop seal to measure the fractions of the fluidizing flow of loop seal that went to each reactor. It was obtained that about the 65% ($\pm 5\%$) of the flow fed into the loop seal goes to the fuel reactor and the rest goes to the air reactor.

To do a deeper study of the carbon capture behavior, the gasification step should be assessed.

The char conversion, X_{char} , is defined as the fraction of carbon in the effective char fed to the fuel reactor which is gasified and thus released to the fuel reactor outgoing gas stream:

$$X_{char} = \frac{[F_{CO_2,FR} + F_{CO,FR} + F_{CH_4,FR} - F_{C,vol}]_{out} - [F_{CO_2,FR}]_{in}}{[F_{CO_2,FR} + F_{CO,FR} + F_{CH_4,FR} + F_{CO_2,AR} - F_{C,vol}]_{out} - [F_{CO_2,FR}]_{in}} = \frac{F_{C,char\ eff} - F_{CO_2,AR}}{F_{C,char\ eff}} \quad (7)$$

The gasified char in the fuel reactor was calculated as difference between the carbon in gases in the fuel reactor outgoing flow, and the carbon flow coming from the volatile matter, $F_{C,vol}$. The carbon content in the volatiles is directly calculated using the ultimate and proximate analysis of coal as the total carbon in coal minus the fixed carbon. $F_{C,char\ eff}$ is the carbon in the effective char flow introduced in the CLC system and is calculated by means of the carbon mass balance in the plant, as it can be deduced from Eq. (7).

An approximation to the char gasification rates can be obtained, if a simplified model is used.

The fuel reactor is considered to follow a continuous stirred-tank reactor (CSTR) model. The char is assumed to be in perfect mixing with the solids in the fuel reactor and to react at a rate ($-r_C$) which is proportional to the mass. With these considerations, ($-r_C$) is calculated from a carbon balance in the fuel reactor:

$$(-r_C) = \frac{1}{m_{\text{char}}} \frac{dm_{\text{char}}}{dt} = k \Rightarrow (-r_C) = \frac{X_{\text{char}} \cdot F_{C,\text{char eff}} \cdot M_C}{m_{\text{char,FR}}} \quad (8)$$

being M_C the carbon molar weight and $m_{\text{char,FR}}$ the mass of carbon in char in the fuel reactor, which can be calculated with the mass of ilmenite in the fuel reactor $m_{\text{ilm,FR}}$, and the solids circulation rate F_{ilm} :

$$\frac{m_{\text{char,FR}}}{m_{\text{ilm,FR}}} = \frac{F_{\text{CO}_2,\text{AR}}}{F_{\text{ilm}}} \quad (9)$$

Besides, the mean residence time of ilmenite, $t_{m,\text{ilm}}$, is calculated by Eq. (10).

$$t_{m,\text{ilm}} = \frac{m_{\text{ilm,FR}}}{F_{\text{ilm}}} \quad (10)$$

The combustion efficiency in the fuel reactor, $\eta_{\text{comb FR}}$, is a measure of gas conversion in the fuel reactor. It is defined as the fraction of the oxygen demanded by the volatile matter and gasification products that is supplied by the oxygen carrier in the fuel reactor. It depends on the reaction rate of ilmenite with the gaseous fuels and on the amount of the reducing gases released by coal in the fuel reactor. The combustion efficiency was calculated as:

$$\eta_{\text{comb FR}} = \frac{[0.5 \cdot F_{\text{H}_2\text{O,FR}} + F_{\text{CO}_2,\text{FR}} + 0.5 \cdot F_{\text{CO,FR}}]_{\text{out}} - [0.5 \cdot F_{\text{H}_2\text{O,FR}} + F_{\text{CO}_2,\text{FR}} + 0.5 \cdot O_{\text{coal,eff}}]_{\text{in}}}{O_{2 \text{ demand coal,eff}} - F_{\text{CO}_2,\text{AR}}} \quad (11)$$

$O_{\text{coal,eff}}$ is the flow of oxygen contained in the effective coal fed. $O_{2 \text{ demand coal,eff}}$ is the oxygen flow needed to fully burn the effective coal flow. The flow of steam from the fuel reactor was calculated from a hydrogen balance in the reactor.

If complete combustion of the gasification products is assumed, a combustion efficiency of the volatile matter, $\eta_{\text{comb vol}}$, can be calculated, as for Eq. (12).

$$\eta_{\text{comb vol}} = \frac{O_{2 \text{ demand gases FR}}}{O_{2 \text{ demand volatiles}}} = \frac{2 \cdot F_{\text{CH}_4,\text{FR}} + 0.5 \cdot F_{\text{H}_2,\text{FR}} + 0.5 \cdot F_{\text{CO,FR}}}{O_{2 \text{ demand volatiles}}} \quad (12)$$

This parameter can give an idea of how much the volatiles of each type of fuel are oxidized since they have poorer contact with the oxygen carrier bed [12].

The oxygen demand, Ω_T , has been also used as an adequate parameter to evaluate the performance of the whole combustion process. It is defined as the fraction of oxygen lacking to achieve a complete combustion to CO_2 and H_2O of the fuel reactor product gas in comparison to the oxygen demand of the effective introduced coal. It is the only fraction of oxygen required in the iG-CLC process to reach full combustion of the fuel that must be supplied in a subsequent polishing step as pure O_2 .

$$\Omega_T = \frac{\text{O}_{2 \text{ demand gases FR}}}{\text{O}_{2 \text{ demand coal,eff}}} = \frac{2 \cdot F_{\text{CH}_4,\text{FR}} + 0.5 \cdot F_{\text{H}_2,\text{FR}} + 0.5 \cdot F_{\text{CO},\text{FR}}}{\text{O}_{2 \text{ demand coal,eff}}} \quad (13)$$

The rate of oxygen transferred by ilmenite, $(-r_{\text{O}})$, is a measure of how much and how fast oxygen is transferred from ilmenite to the fuel. $(-r_{\text{O}})$ is calculated as the oxygen gained in the flow of oxygen-containing gases (CO , CO_2 and H_2O), divided by the ilmenite hold-up:

$$(-r_{\text{O}}) = \frac{([0.5 \cdot F_{\text{H}_2\text{O},\text{FR}} + F_{\text{CO}_2,\text{FR}} + 0.5 \cdot F_{\text{CO},\text{FR}}]_{\text{out}} - [0.5 \cdot F_{\text{H}_2\text{O},\text{FR}} + F_{\text{CO}_2,\text{FR}} + 0.5 \cdot \text{O}_{\text{coal,eff}}]_{\text{in}}) \cdot M_{\text{O}_2}}{m_{\text{ilm,FR}}} \quad (14)$$

4. Results and discussion

The feasibility of using the CLC technology with different fuels was tested, and influence of the type of fuel on the continuous performance was determined. In the literature it was found that the temperature in the fuel reactor is one of the parameters with most influence on coal conversion [10,12,16] because of its effect on the gasification rate. Indeed, the gasification step has high influence on the performance of this process [24-27]. In this work an evaluation of the iG-CLC process performance with different coals was made for increasing fuel reactor temperature. Also different $\text{H}_2\text{O}:\text{CO}_2$ mixtures as gasification agent for all fuels were tested.

Previous experiments done to evaluate the influence of different operational parameters showed that in this process to operate at lower recirculation rates led to an increase in the char conversion and to an enhancement of the system performance [12] because of an increase in the residence times of solids in the fuel reactor. Therefore, the recirculation rates in all these

experiments were set at low values. In these conditions, the resulting oxygen carrier to fuel ratio for all fuels tested was about 1.0-1.1. The oxygen carrier to fuel ratio is a measure of how much oxygen can be supplied by the circulating oxygen carrier compared to the oxygen needed to burn the fuel fed in. Under stoichiometric conditions regarding complete fuel conversion and activated ilmenite this ratio is equal to one.

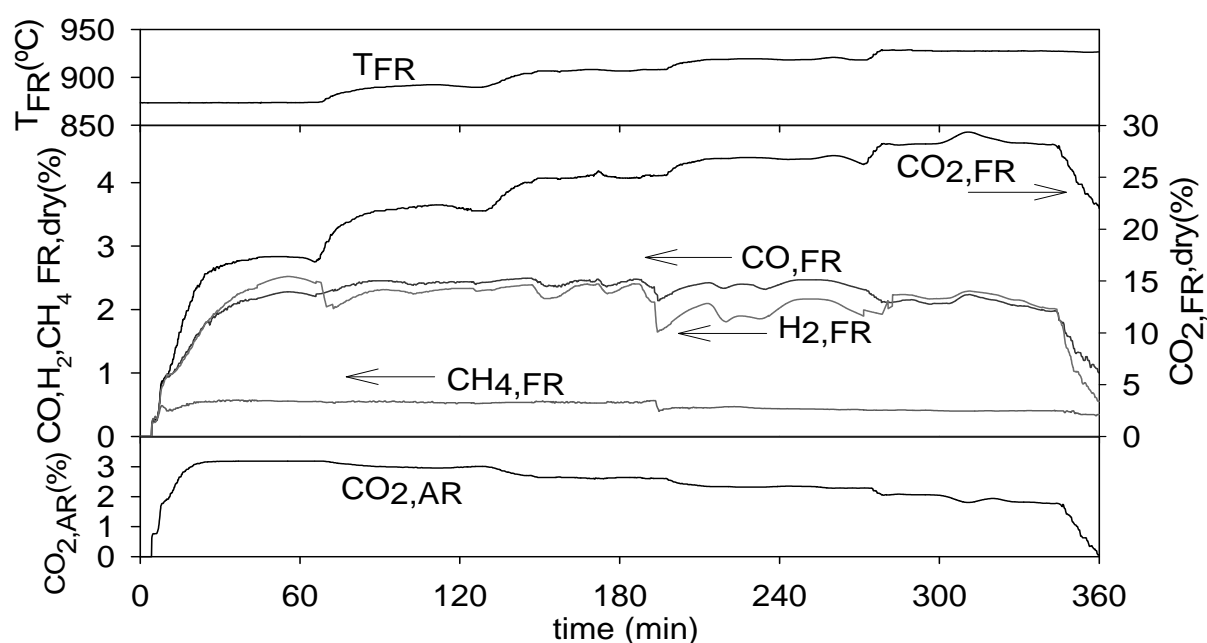


Fig. 3. Evolution with time of the gas concentrations from the fuel reactor (CO, H₂, CH₄ and CO₂) and CO₂ from the air reactor for the experiments using anthracite as fuel with increasing fuel reactor temperature, T_{FR}.

As representative of the gas distributions obtained in this study, the evolution with time of the gas concentrations from the fuel reactor is shown in Fig. 3 for the experiments using anthracite as fuel with increasing fuel reactor temperature, T_{FR}. The initial period before introducing coal and the transitory period until the steady state was reached are also represented. Concentrations in fuel reactor are in dry basis. Steady state after changing the temperature was fast reached and all the points were therefore evaluated at stable conditions.

Similar behavior of the transient period was observed when the type of gasifying gas was changed. The CLC prototype was easy to operate and control with all kinds of fuels, and the steady state for each operating condition was maintained for at least 30 min. Thus, the feasibility of using coals of different rank in an *in-situ* gasification CLC system was proven with this study. The performance of the system according to the characteristics of each fuel is later assessed.

The outlet of the fuel reactor was mainly composed of oxidized CO_2 , and H_2 and CO and some CH_4 as not fully oxidized products of char gasification and volatile matter. Gas chromatography analyses and tars measurements showed that there were neither hydrocarbons heavier than CH_4 nor tars in the fuel reactor outlet flow. Thus, these species were converted in the fuel reactor. The char that was not gasified in the fuel reactor entered into the air reactor and was there burnt with a consequent CO_2 release. The CO_2 concentration in the air reactor is also shown in Fig. 3.

4.1. Effect of the temperature on the iG-CLC performance

Continuous tests were done at different temperatures with each fuel. In this section, results obtained with Spanish lignite within the temperature interval 870-920°C, with MV bituminous South African coal within the temperature interval 850-915°C and a third series of experiments with Spanish anthracite within the temperature interval 870-930°C were done. The coal feeding flows and average temperatures used are gathered in Table 3. In all cases steam was used as gasification agent.

From the concentration of gases exiting the fuel reactor, as it was showed in Fig. 3, the flows of CO_2 , CO , H_2 and CH_4 from the fuel reactor were calculated. Fig. 4 shows the molar flows of CO_2 , CO , H_2 and CH_4 in the fuel reactor outlet for the series of experiments performed at different temperatures and for the fuels tested in this work, that is, Spanish lignite, MV

bituminous South African coal and Spanish anthracite. CO_2 comes mainly from the oxidation of the products of gasification and devolatilization. In case of anthracite, the molar flow of CH_4 is low because this fuel has low fraction of volatiles. The fraction of H_2 , CO and CH_4 for South African coal and Spanish lignite was higher as these fuels have higher fraction of volatile matter. For lignite the CO_2 flow is quite high compared to the other solid fuels, which indicates that the conversion of this fuel in the fuel reactor was higher. As for the effect of the temperature, the trends are the same for all the fuels tested: both gasification and oxidation reactions are promoted with the temperature. Thus the generated CO_2 flow increases with the temperature, whereas the H_2 , CO and CH_4 flows are less affected by temperature.

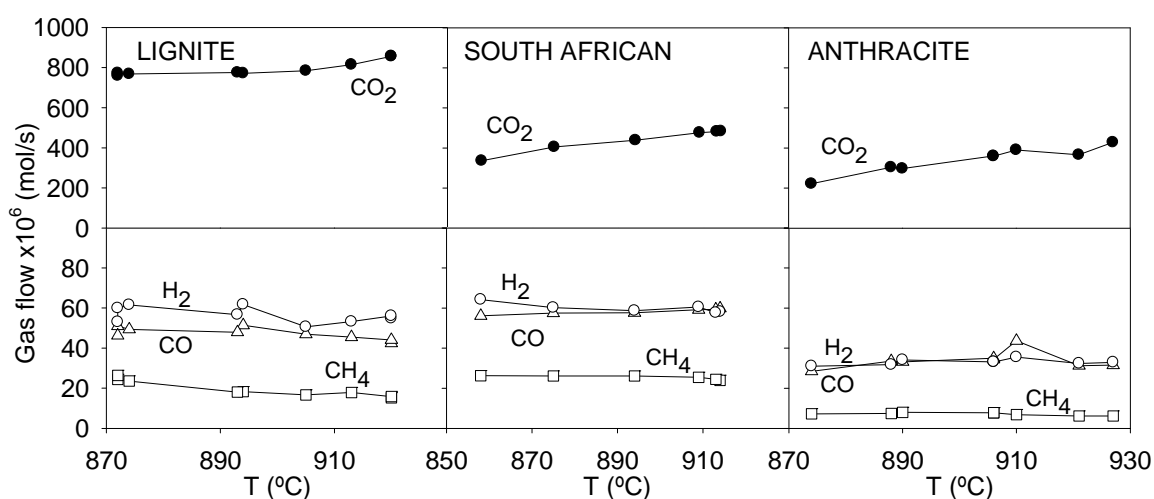


Fig. 4. CO_2 , CO , H_2 and CH_4 molar flows from the fuel reactor at different fuel reactor temperatures with lignite, MV bituminous coal and anthracite. \bullet CO_2 , \blacksquare CO , \circ H_2 and \square CH_4 .

4.1.1. Carbon capture efficiency and char gasification

Fig. 5 shows the carbon capture efficiency obtained for different temperatures for the coals tested. As well, at similar experimental conditions the value obtained for HV bituminous Colombian coal in a previous study is shown. η_{CC} was dependent on coal rank because of the

gasification reactivity of the coal chars. Lignite reached the highest values of η_{CC} , followed by HV bituminous Colombian, MV bituminous South African coal and it was lower for anthracite. Note that this facility has no carbon separation system and higher values could be obtained in a unit if a carbon separation system was incorporated. A theoretical approach supports this statement [38]. Nevertheless, the results obtained in this facility are valuable to evaluate the performance of the iG-CLC technology with different types of coals.

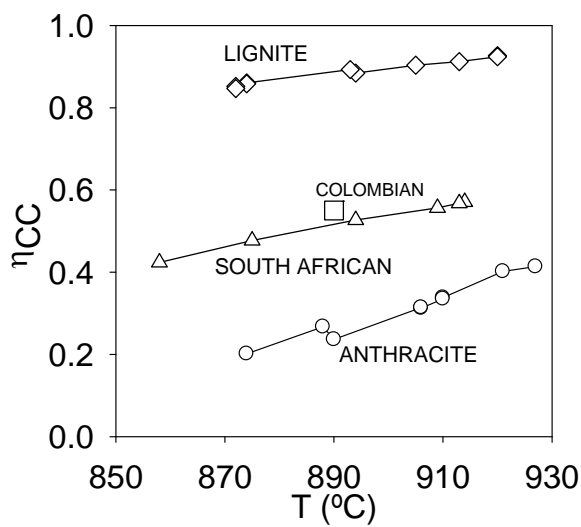


Fig. 5. Carbon capture efficiency variation with the fuel reactor temperature for ◇— lignite, □— HV bituminous Colombian coal, △— MV bituminous South African coal, ○— anthracite. Coal particle size: +200-300 μm .

Since the carbon from the volatiles exits with the fuel reactor outlet stream, that fraction of carbon is always captured. Thus, the carbon capture efficiency depends on the char conversion and on the ratio between the flow of carbon in the volatile matter, $F_{C,\text{vol}}$ and flow of carbon in the introduced char, $F_{C,\text{char eff}}$. This fact can be seen in the following expression for the carbon capture efficiency:

$$\eta_{CC} = \frac{X_{char} \cdot F_{C,char\ eff} + F_{C,vol}}{F_{C,char\ eff} + F_{C,vol}} = \frac{X_{char} + \frac{F_{C,vol}}{F_{C,char\ eff}}}{1 + \frac{F_{C,vol}}{F_{C,char\ eff}}} \quad (15)$$

That is, the char conversion attained and the different content of volatiles in the fuels, or more precisely, the ratio $F_{C,vol}/F_{C,char\ eff}$ of the coal considered, determine the carbon capture efficiency achieved. Only the effective carbon fed is considered in the analysis. Thus, the char elutriated is not taken into account because it is not really involved in the process. The average $F_{C,vol}/F_{C,char\ eff}$ ratios were 0.57 for lignite, 0.35 for Colombian bituminous coal, 0.43 for South African bituminous coal and 0.01 for anthracite.

Fig. 6 represents the char conversions reached at different temperatures for the coals studied. The comparable result for HV bituminous Colombian coal is also shown. Lignite had much higher char conversion than the rest. The char conversion obtained for the other coals are closer, indicating that they have more similar gasification rates, but lower than the gasification rate of lignite [25,28-31].

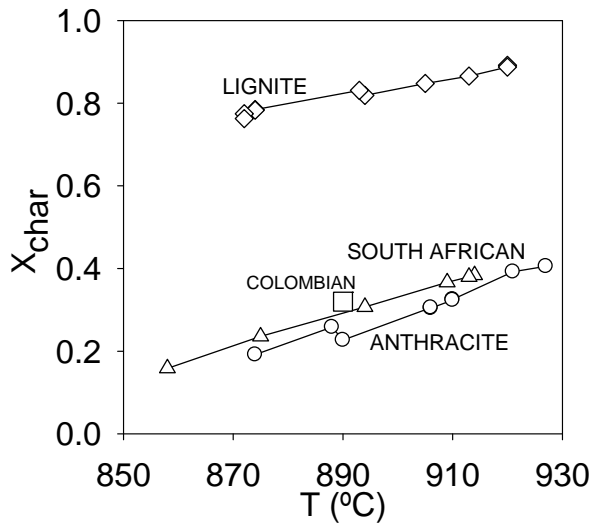


Fig. 6. Char conversion variation with the fuel reactor temperature for \diamond lignite, \square HV bituminous Colombian coal, \triangle MV bituminous South African coal, \circ anthracite. Coal particle size: +200-300 μm .

Both char conversions and carbon capture efficiency for anthracite were similar because the volatile matter fraction is low, whereas for the other coals the values of carbon capture efficiency were higher than values of X_{char} . HV bituminous Colombian and MV bituminous South African coal have similar $F_{\text{C,vol}}/F_{\text{C,char eff}}$ ratios and char conversions reached, so their increase in η_{CC} compared to X_{char} is similar. Nevertheless, for lignite X_{char} and η_{CC} are similar. The mean residence time of char particles in the fuel reactor is a key factor affecting the char conversion [13]. The mean residence time of ilmenite gives an idea of the time that char had to gasify. The resulting mean residence times of ilmenite were 15.5 minutes for lignite, 15.0 minutes for MV bituminous South African coal and 16.6 minutes for anthracite. For the experiment done with HV bituminous Colombian coal it was 14.5 minutes. That is, all experiments with different coals had similar mean residence time of solids. The char conversion reached for anthracite was somewhat lower, which indicates that the gasification rate of anthracite is lower than the rest.

Fig. 7 shows the char conversion rates calculated for all the coals tested at different temperatures, calculated with Eq. 8. As it could be anticipated from the resulting char conversions, at all temperatures anthracite has the lowest char conversion rate, both bituminous coals have similar $(-r_{\text{C}})$, although for HV Colombian is higher, and lignite shows much higher conversion rates compared to the rest. As an example, at 900°C, $(-r_{\text{C}})$ was 31.0%/min for lignite, 4.5%/min for HV bituminous Colombian coal, 3.1%/min for MV bituminous South African coal, 2.2%/min for anthracite. This is also in line with the trend expected from the rank of the coals tested [39].

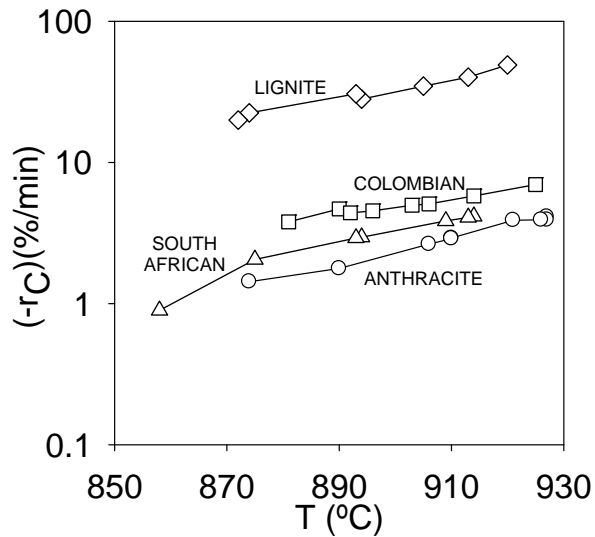


Fig. 7. Rates of char conversion at different fuel reactor temperatures for \diamond lignite, \square HV bituminous Colombian coal, \triangle MV bituminous South African coal, \circ anthracite. Coal particle size: +200-300 μm .

Additional tests in TGA were done to evaluate the conversion of char under well-defined conditions. Fig. 8 shows the variation of char conversion with time reached at 950°C in TGA for the coals used in this study. As it would be expected from the coal ranks, char from lignite has the fastest gasification rate, followed by bituminous Colombian coal char, then bituminous South African coal char and char from anthracite has the slowest gasification rate. The resulting char of the bituminous Colombian coal, due to the mentioned thermal pre-treatment, was somewhat more reactive compared to fresh coal, as it can be seen in Fig. 8. However, this enhancement in the gasification rate was not substantial.

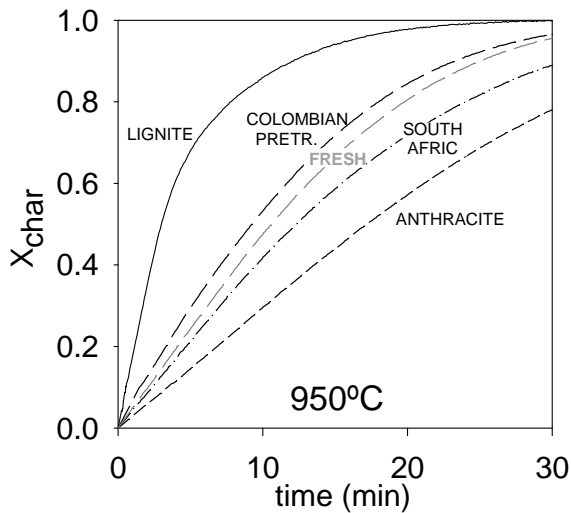


Fig. 8. Char conversion vs. time using a mixture 50% H_2O +50% N_2 as gasification agent done in TGA of char from — lignite, --- pretreated and --- fresh HV bituminous Colombian coal, ---- MV bituminous South African coal and ----- anthracite at 950°C.

Note that the values of char conversion rate obtained in continuous testing are lower than the values obtained in batch fluidized bed experiments [27] or from the above TGA tests. That is because for the continuous tests the supposition that there is perfect mixing was made and the char mass in the fuel reactor considered is probably higher than the real value due to some char segregation at the upper part of the bed. Furthermore, for the calculation of $(-r_C)$ in the continuous tests no inhibition effect is considered.

From these results, it can be concluded that the gasification rates follow the order expected from the rank of the different coals: it is faster for lignite, then HV bituminous coal, MV bituminous coal and it is slower for anthracite.

4.1.2. Combustion efficiency and oxygen demand

The fuel reactor combustion efficiency, $\eta_{comb FR}$, indicates the extent of conversion of the gases released in the fuel reactor, that is, the devolatilization and gasification products, due to the oxidation by ilmenite. Fig. 9 shows $\eta_{comb FR}$ for all fuels tested at the different temperatures. For all the fuels tested, the combustion efficiencies obtained grow slightly with

the temperature because the reaction rate of ilmenite increases with the temperature. The temperature influences the $\eta_{\text{comb FR}}$ of all types of coals in a similar way as the slopes of the curves are similar. The activation energy of the reaction of CH_4 with ilmenite is higher than with H_2 and CO [40], and a coal with high volatile content could be slightly more influenced by the temperature, but the differences are not relevant.

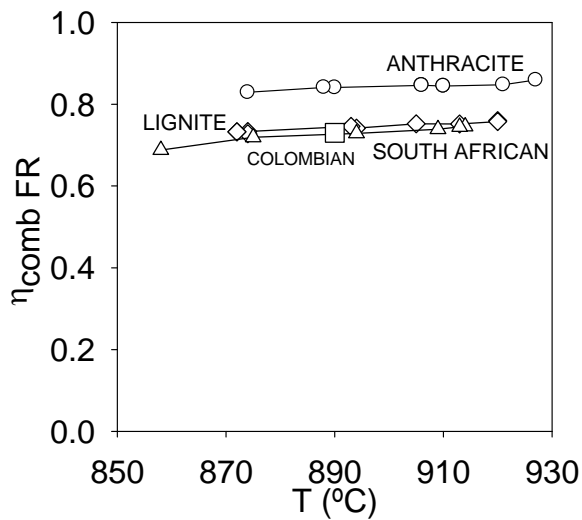


Fig. 9. Fuel reactor combustion efficiency variation with the fuel reactor temperature for \diamond lignite, \square HV bituminous Colombian coal, \triangle MV bituminous South African coal, \circ anthracite. Coal particle size: +200-300 μm .

For all the temperatures tested, $\eta_{\text{comb FR}}$ was higher for anthracite, followed by lignite and MV bituminous South African coal. The test with HV bituminous Colombian coal gave a value of $\eta_{\text{comb FR}}$ slightly higher than with MV bituminous South African coal. In previous experiments it was seen that the released volatiles have worse contact with the oxygen carrier particles and are therefore less converted. On the contrary, gasification products are highly oxidized [12]. This explains the higher $\eta_{\text{comb FR}}$ for anthracite, since the volatile fraction is lower. Lignite has higher fraction of volatile matter compared to South African coal, which could indicate lower $\eta_{\text{comb FR}}$ for lignite. However, the resulting $\eta_{\text{comb FR}}$ for lignite was slightly higher because the

relative fraction of gasification products compared to volatiles was higher due to the fast char gasification rate of lignite. This fact improves the combustion efficiency in the fuel reactor because gasification products are better burnt than volatiles [12]. Besides the solids inventory used in every case could have some influence on the combustion efficiency in the fuel reactor. The solids inventories used were 1770 kg/MW_{th} for lignite, 1580 kg/MW_{th} for Colombian coal, 1380 kg/MW_{th} for South African coal and 1400 kg/MW_{th} for anthracite. Thus, higher combustion efficiency values than expected could be obtained for lignite because the higher solids inventory regarding to the experiments done with other coals. In the other cases, simulations made in a previous work showed that the combustion efficiency increase was of low relevance when the solids inventory increased from 1400 to 1600 kg/MW_{th} [38].

From previous experiments with a HV bituminous Colombian coal, it was concluded that the unconverted H₂, CO and CH₄ in the fuel reactor outlet come from unconverted volatile matter due to its poorer contact with the oxygen carrier particles, whereas gasification products reached full oxidation. Fig. 10 shows the combustion efficiency of volatiles with the different solid fuels at different temperatures, as calculated from Eq. (12). The combustion efficiency of volatiles was lower for lignite than for bituminous coals. The volatile matter of each type of fuel, which is higher for lignite and very similar for both bituminous coals, could affect to the combustion efficiency. On the contrary, lower combustion efficiency of volatiles from anthracite was obtained, although its volatile content was low. This could be explained by means of the composition of volatiles of each type of fuel: the oxygen demanded per mol of volatiles of anthracite is higher than for lignite, then for South African and then for bituminous Colombian coal. This fact could indicate that volatiles from anthracite are more refractory against combustion. In addition, any remarkable trend with the temperature was observed with all type of coals. This fact can be due to the combustion of volatiles depends mainly on the contact between the released volatile matter in a plume and the oxygen carrier

particles in the bed, lowering the relevance of the variation of the oxygen carrier reactivity with temperature. The average of combustion efficiency of volatiles was around 52% for lignite, 61% for HV bituminous Colombian coal, 58% for MV bituminous South African coal, 42% for anthracite.

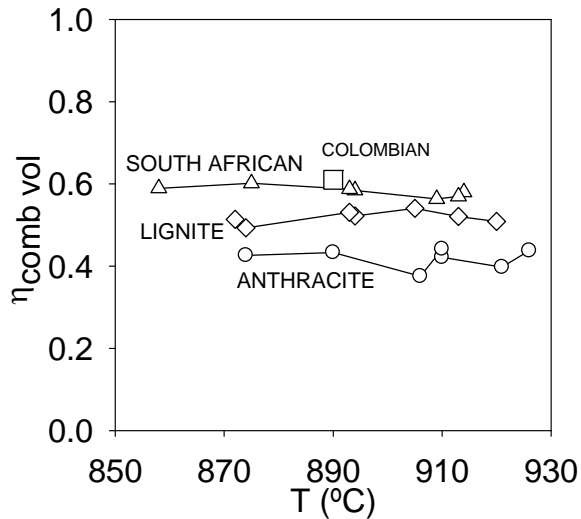


Fig. 10. Combustion efficiency of volatile matter at several fuel reactor temperatures for \diamond lignite, \square HV bituminous Colombian coal, \triangle MV bituminous South African coal, \circ anthracite. Coal particle size: +200-300 μm .

The additional oxygen that would be needed to fully oxidize the outlet gas stream compared to the total oxygen demanded by the fuel fed is the oxygen demand, Ω_T . It represents an extra cost for the process, since an oxygen polishing step would be necessary to fulfill this demand. Fig. 11 shows the oxygen demand of all fuels tested at different temperatures, which turned out to be quite low: it was below 10% in all cases. As mentioned, the oxygen demand is caused by unconverted volatiles at the fuel reactor outlet. The slight decrease of the oxygen demand with the temperature is explained because the oxidation reactions are promoted with the temperature. Ω_T was especially low for anthracite, as it was around 3.5%, because the

volatile fraction in this fuel is low. Bituminous coals have the higher volatile fraction and thereby higher oxygen demand.

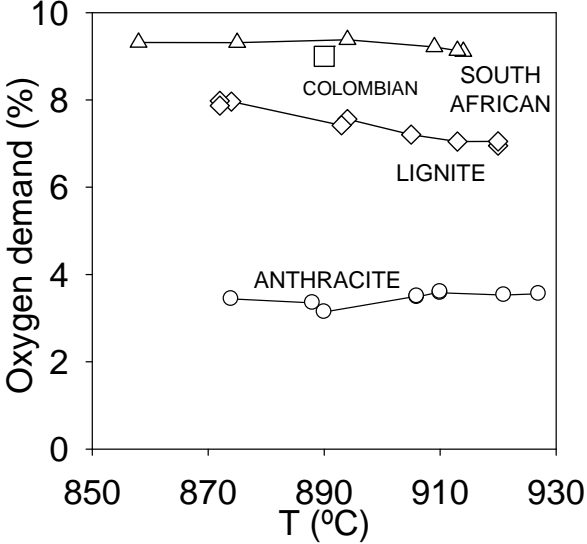


Fig. 11. Oxygen demand variation with the fuel reactor temperature for \diamond lignite, \square HV bituminous Colombian coal, \triangle MV bituminous South African coal, \circ anthracite. Coal particle size: +200-300 μm .

Fig. 12 shows the rate of oxygen transferred by ilmenite, ($-r_{\text{O}}$), for all the fuels tested with increasing temperature. It can be seen that more oxygen was transferred to oxidize the volatiles and the gasification products for increasing temperature for all fuels tested. The transfer of oxygen is limited by the extent of char gasification and the contact of the volatile matter with the oxygen carrier. Nevertheless, the intrinsic reactivity of ilmenite particles is higher than the values showed in Fig. 12 [40]. Thus, the reaction rate of ilmenite increases with the temperature, but the resulting increased oxygen transfer was mainly because char was further gasified at higher temperatures and there were more gasification products which were oxidized. The rate of oxygen transferred in case of lignite was higher because lignite char was further gasified compared to char from other coals and there was therefore higher

amount of gases released that could react with ilmenite. The rate of oxygen transferred for anthracite was lower because its volatiles content is low and lower amount of gasification products were released due to its slower gasification rate. The oxygen transferred for both bituminous coals were similar due to the similar char conversions and combustion efficiencies reached.

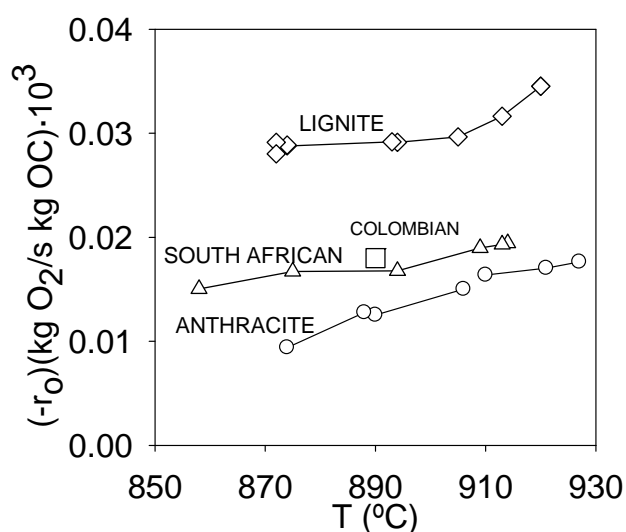


Fig. 12. Oxygen transfer rate variation with the fuel reactor temperature for \diamond lignite, \square HV bituminous Colombian coal, \triangle MV bituminous South African coal, \circ anthracite. Coal particle size: +200-300 μm .

4.2. Effect of the gasification agent type

Since the rate of gasification of the fuel in this process is a determining factor, the effect of using a gas mixture of CO_2 and H_2O on the gasification step and the whole performance of the process with all the fuels considered was evaluated. The motivation of using $\text{H}_2\text{O}-\text{CO}_2$ mixtures as fluidizing gas is that CO_2 can be fed by recirculating a fraction of the product gas stream. Thus, the steam requirements for the gasification would be decreased in some extension, or even avoided if a pure stream of CO_2 was used as fluidizing gas. The coal feeding flows used for the different coals tested, as well as the corresponding average

temperatures are gathered in Table 3. The gasification agent tested for the different fuels were composed of pure steam, pure CO₂ and a CO₂:H₂O mixture around 50:50.

4.2.1. Carbon capture efficiency and char gasification

Fig. 13 shows the carbon capture efficiency and char conversion obtained for the experiments done with different H₂O:CO₂ mixtures as gasification agent. For all fuels tested, the extension of char gasified and carbon capture efficiency decrease for higher CO₂ fraction in the gasification flow. That is because for all the fuels here used the gasification rate is faster with steam than with CO₂. Note that there are some fuels whose gasification rate with CO₂ is fast enough so that it is feasible to use CO₂ as gasification agent [25,29,30]. The decrease in the reached char conversion and η_{CC} when gasifying with higher fraction of CO₂ compared to using pure steam is less pronounced for lignite and higher for anthracite. That is because the char gasification rate with CO₂ is closer to the corresponding rate with steam in case of lignite, and the decrease in the gasification rate is higher in case of anthracite.

When using iG-CLC with some fuels it can be beneficial to use recirculated CO₂ as fluidizing agent in the fuel reactor, as it is the case of lignite. For other fuels to have some CO₂ recirculation can be interesting, as it can be the case of MV bituminous South African coal, which agrees with the results obtained with this fuel in a batch fluidized bed reactor [27]. Similar results were found for HV bituminous Colombian coal [12].

In the experiments with different H₂O:CO₂ mixtures with anthracite the fuel reactor temperature was about 925 °C and with mean solids residence time of 16.6 minutes, whereas with bituminous South African coal they were 910 °C and 15.0 minutes, respectively. This explains that, although char gasification rate with steam is higher for South African coal, the in Fig. 13 represented X_{char} with anthracite and bituminous coal had similar values with CO₂ or H₂O:CO₂ mixtures, or even slightly lower for bituminous coal in case of gasifying with steam. On the other hand, the implementation of an efficient carbon separation system that

increased the char residence time would compensate for any possible disadvantage caused by the slower gasification rate with CO₂.

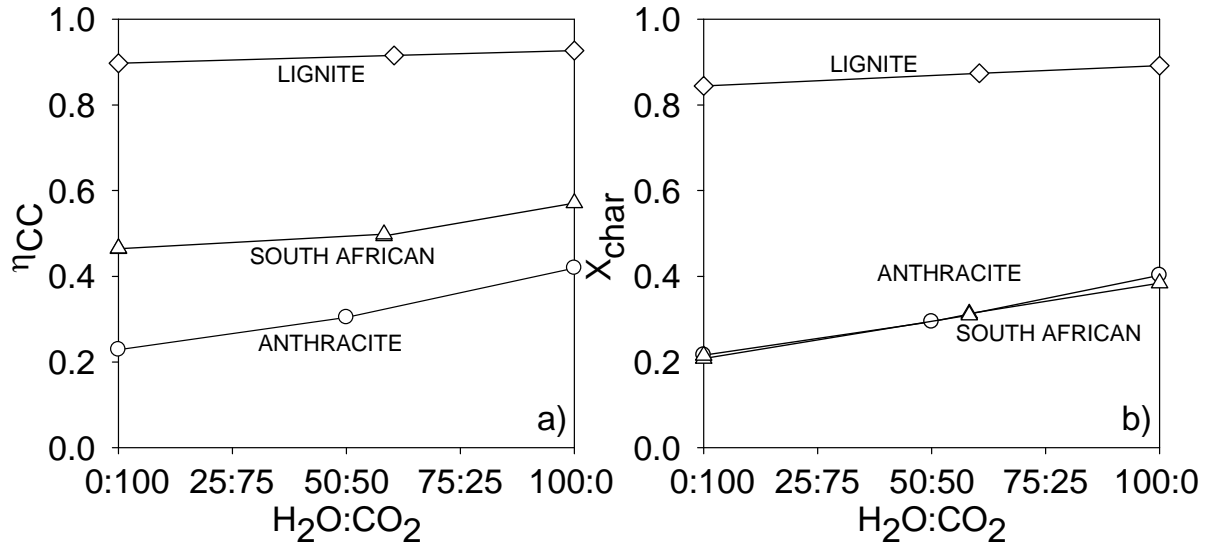


Fig. 13. a) Carbon capture efficiency and b) Char conversion variation for different H₂O:CO₂ mixtures as gasification agent for \diamond lignite, \triangle MV bituminous South African coal, \circ anthracite. Coal particle size: +200-300 μ m. Conditions of experiments: see Table 3.

4.2.2. Combustion efficiency and oxygen demand

Fig. 14 shows the resulting fuel reactor combustion efficiencies and oxygen demands for the experiments done with different H₂O:CO₂ mixtures as gasification agent. It can be seen that both the fuel reactor combustion efficiency and oxygen demand are scarcely influenced by the composition of the gasification agent. When gasifying with higher fraction of CO₂ only CO is produced, whereas when gasifying with H₂O, H₂ is also generated. Although ilmenite reacts faster with H₂ than with CO, the reaction rate of ilmenite is fast enough and the resulting $\eta_{comb FR}$ or Ω_T have no substantial change if the gasification products are enriched in H₂ or CO. As it was calculated by Abad et al. [40], an inventory of 189 kg/MW_{th} would be enough to fully oxidize the generated CO at 900°C, and for H₂ the inventory needed would be even

lower: 66 kg/MW_{th}. However, in these experiments the solids inventories about 1500 kg/MW_{th} are used. As the poor contact between volatiles and oxygen carrier particles is the reason for incomplete combustion even with high solids inventory, the effect of the reactivity of the gas, i.e., H₂ or CO, is of low relevance.

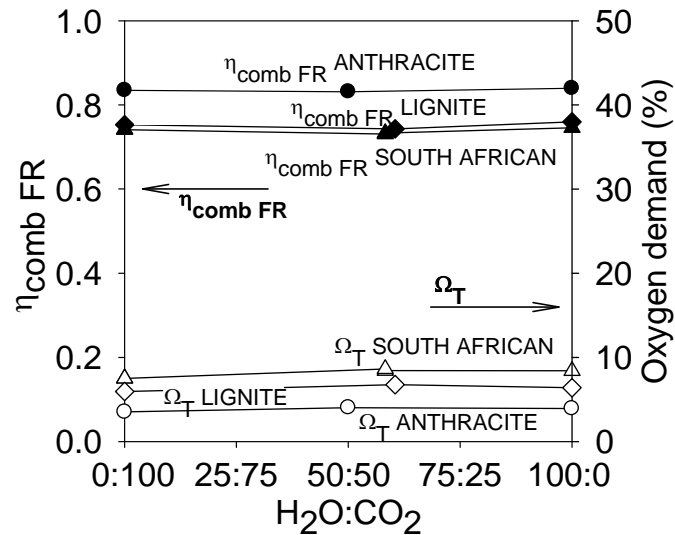


Fig. 14. Fuel reactor combustion efficiency (filled symbols) and oxygen demand (void symbols) variation for different H₂O:CO₂ mixtures as gasification agent for \diamond lignite, \triangle MV bituminous South African coal, \circ anthracite. Coal particle size: +200-300 μ m. Conditions of experiments: see Table 3.

5. Conclusions

The feasibility of using different types of coals with the *in-situ* gasification CLC and the variations in the performance of the process was assessed in a CLC rig for coal when the fuel reactor temperature or the fluidizing gas were changed. The oxygen carrier utilized was ilmenite and a lignite, a high volatile bituminous coal, a medium volatile bituminous coal and a anthracite were used as solid fuels. In this study, the performance of the fuel reactor is evaluated when different types of coals were used.

An increase in the temperature has a beneficial effect on the system performance for all types of coals. The carbon capture efficiency reached is higher for the coals with faster char gasification rates and also when the volatile content in the fuel is higher. High values of carbon capture efficiency, even higher than 90%, can be obtained, but it is essential to have a highly efficient carbon separation system that reintroduced unconverted char particles back to the fuel reactor, especially in case of coals with slow gasification rates such as anthracites. Carbon capture efficiency as high as 93% at 920°C was obtained even without a carbon separation system with lignite, which has a fast char gasification rate.

The combustion efficiency is higher for coals with lower volatile content and for coals with faster gasification rate. The combustion efficiency in the fuel reactor was seen not to be limited by the reaction rate of ilmenite but it is limited by the low conversion of volatile matter. The combustion efficiency of the volatiles seems to depend on the composition of the released volatiles of each type of fuel. The average of combustion efficiency of volatiles was around 52% for lignite, 61% for HV bituminous Colombian coal, 58% for MV bituminous South African coal, 42% for anthracite. Furthermore, in all cases oxygen demands lower than 10% were found, and for anthracite the oxygen demand values were 3.5% because of the lower volatile content of this fuel.

Depending on the type of fuel, some of the steam used as gasification agent can be replaced by CO₂ recirculated from the outlet fuel reactor flow, getting similar system performance and thereby saving energy derived from steam generation. In case of lignite, there is no change in the process performance when gasifying with CO₂. On the other hand, for anthracite the lower gasification rate of char with CO₂ leads to a substantial drop in the performance.

The results show that this technology has the potential to be used to carry out combustion with inherent CO₂ separation using highly reactive coals.

Acknowledgments

This work was partially supported by the Spanish Ministry of Science and Innovation (Project ENE2010-19550). A. Cuadrat thanks CSIC for the JAE Predoc. fellowship belonging to the “Junta para la Ampliación de Estudios” Program and partially supported by the European Social Fund.

Nomenclature

$F_{C, \text{char, eff}}$ carbon flow in the effective char fed (mol/s)

$F_{\text{CO}_2 \text{ AR}}$ carbon flow from the char that goes to the air reactor (mol/s)

$F_{C \text{ vol}}$ carbon flow coming from the volatile matter fed (mol/s)

$F_{i, \text{FR}}$ flow in the fuel reactor of the corresponding gas i (mol/s)

F_{ilm} solids circulation rate (kg/s)

k constant value of the char gasification rate (s^{-1})

M_C carbon molar weight (kg/mol)

$m_{\text{char, FR}}$ mass of char in the fuel reactor (kg)

$m_{\text{ilm, FR}}$ fuel reactor bed mass or solid hold-up in the fuel reactor (kg)

M_{O_2} oxygen molecular weight (kg/mol)

$O_{\text{coal, eff}}$ flow of oxygen contained in the effective coal introduced (moles O/s)

$O_{2 \text{ demand coal, eff}}$ oxygen demand of the effective coal fed (moles O_2/s)

$O_{2 \text{ demand gases, FR}}$ oxygen demand of the fuel reactor outlet flow (moles O_2/s)

$(-r_C)$ char gasification rate (s^{-1})

$(-r_O)$ rate of oxygen transferred by the oxygen carrier (kg O_2/s kg OC)

T_{FR} temperature in the fuel reactor ($^{\circ}\text{C}$)

$t_{\text{m, char}}$ mean residence time of char (s)

$t_{\text{m, ilm}}$ mean residence time of ilmenite (s)

η_{CC} carbon capture efficiency

$\eta_{comb FR}$ fuel reactor combustion efficiency

$\eta_{comb vol}$ combustion efficiency of the volatile matter

X_{char} char conversion

Ω_T total oxygen demand

References

- [1] NOAA-ESRL, 2010. National Oceanic and Atmospheric Administration in the US. Average concentration of CO₂ in the atmosphere (Mauna Loa Observatory) for 2010 was posted September 8, 2011.
- [2] IPCC special report on carbon dioxide capture and storage, Cambridge, UK: Cambridge University Press. 2005.
- [3] International Energy Agency (IEA). Energy technology perspectives: Scenarios and strategies to 2050. Paris, France: OECD/IEA. 2006.
- [4] L.I. Eide, M. Anheden, A. Lyngfelt, C. Abanades, M. Younes, D. Clodic. Novel Capture Processes. Oil Gas Sci. Technol., 60 (2005), pp. 497-508.
- [5] A. Lyngfelt, B. Leckner, T. Mattisson. A fluidized-bed combustion process with inherent CO₂ separation; Application of chemical-looping combustion. Chem. Eng. Sci. 56 (2001), pp. 3101-3113.
- [6] S. Noorman, F. Gallucci, M. van Sint Annaland, J.A.M. Kuipers, A theoretical investigation of CLC in packed beds. Part 1: Particle model. Chem. Eng. J., 167 (2011), pp. 297-307.
- [7] S. Noorman, F. Gallucci, M. van Sint Annaland, J.A.M. Kuipers, A theoretical investigation of CLC in packed beds. Part 2: Reactor model. Chem. Eng. J., 167 (2011), pp. 369-376.

- [8] N. Berguerand, A. Lyngfelt. The use of petroleum coke as fuel in a 10 kWth chemical-looping combustor. *Int. J. Greenhouse Gas Control*, 2 (2008), pp. 169-179.
- [9] N. Berguerand, A. Lyngfelt. Design and operation of a 10 kWth chemical-looping combustor for solid fuels – Testing with South African coal. *Fuel*, 87 (2008), pp. 2713-2726.
- [10] N. Berguerand, A. Lyngfelt. Chemical-Looping combustion of petroleum coke using ilmenite in a 10 kWth unit-high-temperature operation. *Energy Fuels*, 23 (2009), pp. 5257-5268.
- [11] N. Berguerand, A. Lyngfelt. Operation in a 10 kWth chemical-looping combustor for solid fuel—Testing with a Mexican petroleum coke. *Energy Procedia*, 1(2009), pp. 407-414.
- [12] A. Cuadrat, A. Abad, F. García-Labiano, P. Gayán, L.F. de Diego, J. Adánez. The use of ilmenite as oxygen carrier in a 500 Wth Chemical-Looping Coal Combustion unit. *Int. J. Greenhouse Gas Control*, 5 (2011), pp. 1630-1642.
- [13] A. Cuadrat, A. Abad, F. García-Labiano, P. Gayán, L.F. de Diego, J. Adánez. Effect of operating conditions in Chemical-Looping Combustion of coal in a 500 Wth unit. *Int. J. Greenhouse Gas Control*, 6 (2012), pp. 153-163.
- [14] L. Shen, J. Wu, J. Xiao. Experiments on chemical looping combustion of coal with a NiO based oxygen carrier. *Combust. Flame*, 156 (2009), pp. 721-728.
- [15] L. Shen, J. Wu, Z. Gao, J. Xiao. Reactivity deterioration of NiO/Al₂O₃ oxygen carrier for chemical looping combustion of coal in a 10 kWth reactor. *Combust Flame*, 156 (2009), pp. 1377-1385.
- [16] L. Shen, J. Wu, Z. Gao, J. Xiao. Characterization of chemical looping combustion of coal in a 1 kWth reactor with a nickel-based oxygen carrier. *Combust Flame*, 157 (2010), pp. 934-942.

- [17] J. Wu, L. Shen, J. Hao, H. Gu. Chemical looping combustion of coal in a 1 kWth reactor with iron ore as an oxygen carrier. Proc 1st Int Conf on Chemical Looping. Lyon, France; 2010.
- [18] Y. Cao, B. Casenas, W.P. Pan. Investigation of Chemical-Looping Combustion by Solid Fuels. 2. Redox Reaction Kinetics and Product Characterization with Coal, Biomass, and Solid Waste as Solid Fuels and CuO as an Oxygen carrier. Energy Fuels, 20 (2006), pp. 1845-1854.
- [19] J. Adánez, A. Abad, F. García-Labiano, P. Gayán, L.F. De Diego. Progress in chemical-looping combustion and reforming technologies Progress in Energy and Combustion Science 38 (2012), pp. 215-282.
- [20] H. Leion, A. Lyngfelt, M. Johansson, E. Jerndal, T. Mattisson. The use of ilmenite as an oxygen carrier in chemical-looping combustion. Chem. Eng. Res. Des., 86 (2008), pp. 1017-1026.
- [21] T. Mendiara, A. Abad, L.F. de Diego, F. García-Labiano, P. Gayán, J. Adánez. Use of a Fe-based residue from alumina production as oxygen carrier in chemical-looping combustion. Energy Fuels (2011), doi: 10.1021/ef201458v.
- [22] H. Leion, E. Jerndal, B.M. Steenari, S. Hermansson, M. Israelsson, E. Jansson, M. Johnsson, R. Thunberg, A. Vadenbo, T. Mattisson, A. Lyngfelt. Solid fuels in chemical-looping combustion using oxide scale and unprocessed iron ore as oxygen carriers. Fuel, 88 (2009), pp. 1945-1954.
- [23] N. Ding, Y. Zheng, C. Luo, Q. Wu, P. Fu, C. Zheng. Development and performance of binder-supported CaSO₄ oxygen carriers for chemical looping combustion. Chem. Eng. J., 171 (2011), pp. 1018-1026.

- [24] J.S. Dennis, S.A. Scott, A.N. Hayhurst. In situ gasification of coal using steam with chemical looping: a technique for isolating CO₂ from burning a solid fuel. *J. Energy Inst.*, 79 (2006), pp. 187-190.
- [25] S.A. Scott, J.S. Dennis, A.N. Hayhurst, T. Brown. In situ gasification of a solid fuel and CO₂ separation using chemical looping. *AIChE J*, 52 (2006), pp. 3325-3328.
- [26] H. Leion, T. Mattisson, A. Lyngfelt. The use of petroleum coke as fuel in chemical-looping combustion. *Fuel*, 86 (2007), pp. 1947-1958.
- [27] A. Cuadrat, A. Abad, J. Adánez, L.F. de Diego, F. García-Labiano, P. Gayán. Prompt Considerations on the Design of Chemical-Looping Combustion of Coal from Experimental Tests. *Fuel*. doi: 10.1016/j.fuel.2012.01.050.
- [28] H. Leion, T. Mattisson, A. Lyngfelt. Solid fuels in chemical-looping combustion. *Int. J. Greenhouse Gas Control*, 2 (2008), pp. 180-193.
- [29] J.S. Dennis, S.A. Scott. In situ gasification of a lignite coal and CO₂ separation using chemical looping with a Cu-based oxygen carrier. *Fuel*, 89 (2010), pp. 1623-1640.
- [30] J.S. Dennis, C.R. Müller, S.A. Scott. In situ gasification and CO₂ separation using chemical looping with a Cu-based oxygen carrier: Performance with bituminous coals. *Fuel*, 89 (2010), pp. 2353-64.
- [31] C. Linderholm, A. Cuadrat, A. Lyngfelt. Chemical-Looping combustion of solid fuels in a 10 kWth pilot – batch tests with five fuels. *Energy Procedia*, 4 (2011), pp. 385-92.
- [32] L. Shen, J. Wu, J. Xiao, Q. Song, R. Xiao. Chemical-Looping Combustion of Biomass in a 10 kWth Reactor with Iron Oxide as an Oxygen carrier. *Energy Fuels*, 23 (2009), pp. 2498-2505.
- [33] H. Gu, L. Shen, J. Xiao, S. Zhang, T. Song. Chemical Looping Combustion of Biomass/Coal with Natural Iron Ore as Oxygen Carrier in a Continuous Reactor. *Energy Fuels*, 25(2011), pp. 446–455.

- [34] A.R. Bidwe, F. Mayer, C. Hawthorne, A. Charitos, A. Schuster, G. Scheffknecht. Use of ilmenite as an oxygen carrier in Chemical-Looping Combustion – Batch and continuous dual fluidized bed investigation. *Energy Procedia*, 2011, 4, 433-440.
- [35] A. Cuadrat, A. Abad, J. Adánez, L.F. de Diego, F. García-Labiano, P. Gayán. Behavior of Ilmenite as Oxygen carrier in Chemical-Looping Combustion. *Fuel Proc. Tech.* 94 (2012), pp. 101-112.
- [36] J. Adánez, A. Cuadrat, A. Abad, P. Gayán, L.F. de Diego, F. García-Labiano. Ilmenite Activation during Consecutive Redox Cycles in Chemical-Looping Combustion. *Energy Fuels*, 24 (2010), pp. 1402-1413.
- [37] P. Simell, P. Stahlberg, E. Kurkela, J. Albretch, S. Deutch, K. Sjostrom. Provisional protocol for the sampling and analysis of tar and particulates in the gas from large-scale biomass gasifiers. Version 1998. *Biomass and Bioenergy*, 18(2000), pp. 19-38.
- [38] A. Cuadrat, A. Abad, P. Gayán, L.F. de Diego, F. García-Labiano, J. Adánez. Theoretical approach on the CLC performance with solid fuels: optimizing the solids inventory. *Fuel*. doi: 10.1016/j.fuel.2012.01.071.
- [39] J.L. Johnson. Fundamentals of Coal Gasification. In *Chemistry of coal utilization*. 2nd supplementary volume. Chapter 23. Ed. M.A. Elliott. Wiley-Interscience Publication, New York, 1981.
- [40] A. Abad, J. Adánez, A. Cuadrat, F. García-Labiano, P. Gayán, L.F. de Diego. Reaction kinetics of ilmenite for Chemical-Looping Combustion. *Chem. Eng. Sci.*, 66 (2011), pp. 689-702.